Fully Coupled Numerical Methods for Elastohydrodynamic Lubrication Line Contact Problems by the High Order Finite Difference Methods

QUAN SHEN
Soochow University
Bing Wu (jiaoda-wubing@163.com)
Soochow University
GUANGWEN XIAO
Soochow University

Research Article

Keywords: Elastohydrodynamic lubrication, Line contact problems, High or- der nite di erence methods, Trust-region dogleg algorithm

Posted Date: September 24th, 2021

DOI: https://doi.org/10.21203/rs.3.rs-914621/v1

FULLY COUPLED NUMERICAL METHODS FOR ELASTOHYDRODYNAMIC LUBRICATION LINE CONTACT PROBLEMS BY THE HIGH ORDER FINITE DIFFERENCE METHODS

QUAN SHEN*, BING WU† AND GUANGWEN XIAO◊

Abstract. In this paper a high order finite difference method is constructed to solve the elastohydrodynamic lubrication line contact problems, whose cavitation condition is handled by the penalty method. The highly nonlinear equations from the discretization of the high order finite difference method are solved by the trust-region dogleg algorithm. In order to reduce the numerical dissipation and dispersion brought by the high order upwind finite difference scheme, a high order biased upwind finite difference scheme is also presented. Our method is found to achieve more accurate solutions using just a small number of nodes compared to the multilevel methods combined with the lower order finite difference method.

Keywords: Elastohydrodynamic lubrication; Line contact problems; High order finite difference methods; Trust-region dogleg algorithm

1. Introduction

Elastohydrodynamic lubrication (EHL) has been widely found in the common high stressed tribology pairs of the mechanical components, such as rolling gears and bearings, in order to reduce the friction and wear between the two contact bodies. For instance, the engineering application of EHL theory has been used in the railway industry, which investigated the wheel/rail contact behavior of high-speed train under rainy days. The thin lubricant film between wheel and rail interfaces has significant effect on the wheel/rail adhesion, which reduces the traction and braking ability of the high-speed train [1]. In addition, the rolling contact of the two components has complex geometric profiles and high wheel/rail axle load resulting in high contact pressures. The high contact pressures and low viscosity of water can have the effect on the elastic deformation and the astringency of the nonlinear solutions of the Reynolds equations. Therefore, a robust and accurate numerical method for the EHL solution should be proposed.

The most popular numerical method for EHL problems is the low order finite difference method combined with the multilevel method [2, 3] due to its efficiency and stability. Interested readers could refer to the review of numerical methods for EHL contact problems in [4]. Our numerical method is based on the high order finite difference method and the state-of-the-art nonlinear solver. In recent years the high order difference method [5] has become a popular choice for solving partial differential equations. As far as we know, there is no research about the

Date: September 15, 2021.

†Corresponding author. This work was supported by the National Natural Science Foundation of China (No. 11401416 and No. 51605318).

high order finite difference method for EHL line contact problems. The traditional low order finite difference method combined with an out-of-date nonlinear solver, e.g., Newton-Raphson solver, suffers extremely poor convergence especially at high load conditions. In this paper, we shall construct a high order centred and (biased) upwind finite difference method combined with a state-of-the-art nonlinear solver, i.e., the trust-region dogleg algorithm, to solve the EHL line contact problems. In addition, there is no need to update the pressure distribution [6] or the cavitation position [6, 7] in our method. Therefore, our method is a fully coupled method.

This paper is organized as follows. The mathematical model of EHL line contact problems is presented in Section 2. In Section 3, we construct the high order finite difference method combined with the trust-region dogleg algorithm to solve the EHL line contact problems. Numerical examples illustrate the high accuracy and stability of our method in Section 4. The last section is a brief conclusion.

2. Mathematical model

In this section, we consider the elastohydrodynamic lubrication (EHL) line contact problems which consist of three equations: the Reynolds equation, the film thickness equation and the force balance equation.

The non-dimensional Reynolds equation is

$$-\frac{d}{dX}\left(\varepsilon\frac{dP}{dX}\right)+\frac{d(\rho H)}{dX}=0, \tag{2.1}$$

$$P(X_{in})=P(X_{out})=0, \tag{2.2}$$

$$P\geqslant 0 \text{ on } [X_{in},X_c], P=0 \text{ on } [X_c,X_{out}], P(X_c)=\frac{dP}{dX}(X_c)=0, \tag{2.3}$$

where $\varepsilon=\frac{\rho H^3}{\lambda\eta}$, λ is a dimensionless speed parameter, $P(X)$ and $H(X)$ are the unknown pressure and film thickness, respectively. The domain of this equation is $[X_{in},X_{out}]$, where X_{in} is the known inlet point, X_{out} is the known outlet point and $X_c\in[X_{in},X_{out}]$ is the unknown cavitation point, which should be solved as a part of the numerical methods. The viscosity and the density are denoted by $\eta(P)$ and $\rho(P)$, the relationship of which to pressure are established by Roelands [8] and Dowson et al. [9], respectively, i.e.,

$$\eta(P)=e^{\frac{\alpha p_0}{z}[-1+(1+\frac{Pp_h}{p_0})^z]}, \tag{2.4}$$

$$\rho(P)=\frac{0.59\times 10^9+1.34Pp_h}{0.59\times 10^9+Pp_h}, \tag{2.5}$$

where z,α,p_0,p_h are the viscosity index, the pressure viscosity index, the ambient pressure and the maximum Hertzian pressure, respectively.

The non-dimensional film thickness equation is given as

$$H(X)=H_{00}+\frac{X^2}{2}-\frac{1}{\pi}\int_{X_{in}}^{X_c}\ln|X-X'|P(X')dX', \tag{2.6}$$

where H_{00} is the unknown central offset film thickness.

The third equation is the non-dimensional force balance equation, i.e.,

$$\int_{X_{in}}^{X_c} P(X)dX = \frac{\pi}{2}. \tag{2.7}$$

Since $P = 0$ on $[X_c, X_{out}]$ in (2.3), we have

$$H(X) = H_{00} + \frac{X^2}{2} - \frac{1}{\pi}\int_{X_{in}}^{X_{out}} \ln|X - X'|P(X')dX', \tag{2.8}$$

$$\int_{X_{in}}^{X_{out}} P(X)dX = \frac{\pi}{2}. \tag{2.9}$$

3. Fully coupled high order finite difference methods

The traditional numerical scheme for the non-dimensional Reynolds equation (2.1), (2.2), (2.3) is the low order finite difference methods (e.g. See [10, 11, 2, 3]). In this section, we shall present the high order (e.g., the fourth-order) centered finite difference scheme to approximate $\frac{d}{dX}$ in the first term in (2.1). And the high order (e.g., the fourth-order) upwind finite difference scheme, which could overcome the spurious oscillations in the numerical treatment of the convection-dominated Reynolds equation (2.1), are proposed to approximate $\frac{d}{dX}$ in the second term in (2.1). Because the high order upwind finite difference scheme will bring the numerical dissipation and dispersion, we also present a high order (e.g., the fourth-order) biased upwind finite difference scheme to reduce them.

We choose N equidistant nodes on $[X_{in}, X_{out}]$, i.e., $X_{in} = X_1 < X_2 < \cdots < X_{N-1} < X_N = X_{out}$, $h = (X_{out} - X_{in})/(N-1)$. The high order centered and upwind finite difference methods can be constructed by the Taylor series. The mathematical details of these high order finite difference approximations can be seen in [12]. These high order schemes have been already programmed in [12] or the Differentiation in Space Subroutines (DSS) library [13], which can be used to approximate $\frac{d}{dX}$ in the first term or the second term in (2.1) in our numerical algorithms directly. For instance, the fourth-order centered finite difference scheme

$$\left.\frac{dP}{dX}\right|_{X=X_i} = \frac{P(X_{i-2}) - 8P(X_{i-1}) + 8P(X_{i+1}) - P(X_{i+2})}{12h}. \tag{3.1}$$

The fourth-order upwind finite difference scheme

$$\left.\frac{d(\rho H)}{dX}\right|_{X=X_i} = \frac{3\rho H(X_{i-4}) - 16\rho H(X_{i-3}) + 36\rho H(X_{i-2}) - 48\rho H(X_{i-1}) + 25\rho H(X_i)}{12h} \tag{3.2}$$

for the lubricants from left to right, where $\rho H(X) := \rho(P(X))H(X)$. For the lubricants from right to left, the fourth-order upwind finite difference scheme can be constructed in an analogous way, i.e.,

$$\left.\frac{d(\rho H)}{dX}\right|_{X=X_i} = \frac{-25\rho H(X_i) + 48\rho H(X_{i+1}) - 36\rho H(X_{i+2}) + 16\rho H(X_{i+3}) - 3\rho H(X_{i+4})}{12h}. \tag{3.3}$$

It is known to all that the upwind finite difference scheme will bring the numerical dissipation and dispersion. In order to reduce them, the fourth-order biased upwind finite difference scheme [14, 15]

(3.4)
$$\left.\frac{d(\rho H)}{dX}\right|_{X=X_i} = \frac{-\rho H(X_{i-3}) + 6\rho H(X_{i-2}) - 18\rho H(X_{i-1}) + 10\rho H(X_i) + 3\rho H(X_{i+1})}{12h}$$

is also proposed to approximate $\frac{d}{dX}$ in the second term in (2.1) for the lubricants from left to right or

(3.5)
$$\left.\frac{d(\rho H)}{dX}\right|_{X=X_i} = \frac{-3\rho H(X_{i-1}) - 10\rho H(X_i) + 18\rho H(X_{i+1}) - 6\rho H(X_{i+2}) + \rho H(X_{i+3})}{12h}$$

for the lubricants from right to left.

It is worth noting that the one-sided high order finite difference schemes are used near the boundary (See [12] or [16] for details), i.e, no fictitious points outside the domain are used in the high order finite difference schemes. Let $\boldsymbol{D_4^c, D_4^u, D_4^{bu}}$ be the $N\times N$ differentiation matrices of the fourth-order centered, upwind and biased upwind finite difference scheme for the first derivative approximation, respectively. Therefore, (2.1) can be rewritten as

$$-\boldsymbol{D_4^c}(\boldsymbol{\varepsilon} * \boldsymbol{D_4^c P}) + \boldsymbol{D_4^u \rho H} = \boldsymbol{0} \tag{3.6}$$

or

$$-\boldsymbol{D_4^c}(\boldsymbol{\varepsilon} * \boldsymbol{D_4^c P}) + \boldsymbol{D_4^{bu} \rho H} = \boldsymbol{0}, \tag{3.7}$$

where

$$\boldsymbol{P} = (P(X_1)\ P(X_2)\ \cdots\ P(X_N))^T, \tag{3.8}$$

$$\boldsymbol{\rho H} = (\rho(P(X_1))H(X_1)\ \rho(P(X_2))H(X_2)\ \cdots\ \rho(P(X_N))H(X_N))^T \tag{3.9}$$

$$\boldsymbol{\varepsilon} = (\varepsilon(X_1)\ \varepsilon(X_2)\ \cdots\ \varepsilon(X_N))^T \tag{3.10}$$

$$\varepsilon(X_i) = \frac{\rho(X_i)H^3(X_i)}{\lambda\eta(X_i)},\ i = 1, 2, \cdots, N. \tag{3.11}$$

The symbol $*$ represents the element-wise multiplication.

Remark 3.1. *For simplicity, we only present the fourth-order centered and (biased) upwind finite difference scheme in the section. However, other high order (e.g., sixth-order or eighth-order) finite difference scheme can be constructed in an analogous way.*

Another difficulty in (2.1), (2.2) and (2.3) is how to deal with the cavitation condition (2.3). A simple and straightforward way to overcome this difficulty is the penalty method [17], which adds a penalty term into (2.1). It becomes

$$-\frac{d}{dX}\left(\varepsilon\frac{dP}{dX}\right) + \frac{d(\rho H)}{dX} + \frac{1}{\xi}\min(P, 0) = 0, \tag{3.12}$$

$$P(X_{in}) = P(X_{out}) = 0, \tag{3.13}$$

where ξ is an arbitrary small positive number.

The discrete scheme for (3.12) and (3.13) is

$$-\frac{d}{dX}\left(\varepsilon\frac{dP}{dX}\right)\bigg|_{X=X_i}+\frac{d(\rho H)}{dX}\bigg|_{X=X_i}+\frac{1}{\xi}\min(P(X_i),0)=0,\ i=2,\cdots,N-1 \tag{3.14}$$

$$P(X_1)=P(X_N)=0. \tag{3.15}$$

The non-dimensional film thickness equation (2.8) could be approximated by the same way in Appendix B of [2], i.e.,

$$H(X_i)=H_{00}+\frac{X_i^2}{2}-\frac{1}{\pi}\int_{X_1}^{X_N}\ln|X_i-X'|P(X')dX' \tag{3.16}$$

$$=H_{00}+\frac{X_i^2}{2}-\frac{1}{\pi}\sum_{j=1}^{N}K_{ij}^{hh}P(X_j), \tag{3.17}$$

where

$$K_{ij}^{hh}=(X_i-X_j+\frac{h}{2})(\ln|X_i-X_j+\frac{h}{2}|-1)-(X_i-X_j-\frac{h}{2})(\ln|X_i-X_j-\frac{h}{2}|-1). \tag{3.18}$$

The non-dimensional force balance equation (2.9) could be approximated by the compound trapezoidal formula, i.e.,

$$\frac{h}{2}\sum_{i=1}^{N-1}(P(X_i)+P(X_{i+1}))-\frac{\pi}{2}=0. \tag{3.19}$$

Let $\boldsymbol{U}=(P(X_1)\ P(X_2)\ \cdots P(X_N)\ H(X_1)\ H(X_2)\cdots H(X_N)\ H_{00})^T$ be the $(2N+1)\times 1$ unknown vector. To summarize, we obtain the nonlinear equations

$$\boldsymbol{F}(\boldsymbol{U})=\mathbf{0}. \tag{3.20}$$

(3.20) are the highly nonlinear equations, which could be solved by the trust-region dogleg algorithm [18]. This algorithm is a variant of the Powell dogleg method [19]. This algorithm has already been implemented in a built-in function 'fsolve' in MATLAB.

4. Numerical Examples

In this section, we shall give several numerical examples to demonstrate the high accuracy of our numerical method. Let M and L be dimensionless load parameter (Moes) and dimensionless materials parameter (Moes), respectively. Then

$$p_h=\frac{L}{\alpha}\sqrt{\frac{M}{2\pi}},\lambda=\frac{3\pi^2}{8M^2}.$$

In these numerical examples, $z = 0.68, \alpha = 1.7 \times 10^{-8}, p_0 = 1.98 \times 10^8, X_{in} = -4, X_{out} = 1.5$, $\xi = 10^{-5}$. The initial guesses of $P(X_i), H(X_i), H_{00}$ in the trust-region dogleg algorithm are as follows:

$$P(X_i) = \begin{cases} \sqrt{1 - X_i^2}, & \text{if } |X_i| < 1, \\ 0, & \text{if } |X_i| \geqslant 1, \end{cases} \tag{4.1}$$

$$H(X_i) = X_i^2/2, \; i = 1, \cdots, N, \tag{4.2}$$

$$H_{00} = 0. \tag{4.3}$$

4.1. **High loads.** Usually, the case of high loads is used to test the reliability of the numerical methods for the EHL line contact problems. Let $M = 200$ and $L = 10$. At this situation, the maximum Hertzian dry contact pressure is 3.3 GPa for $\alpha = 1.7 \times 10^{-8}$. The pressure profile obtained by the biased upwind fourth-order finite difference scheme with $N = 4001$ is in Figure 1. In the line contact pressure profiles, there is a very local maximum close to the outlet first showed by Petrusevich [20]. Generally speaking, this phenomenon is caused by the exponential relation, e.g., (2.4) between viscosity and pressure. The numerical results of the pressure spike (P_s) and the minimum film thickness (H_m) are in Table 1 and Table 2. From Table 1 and Table 2, we find that both upwind and biased upwind finite difference schemes have much more accuracy than other methods in [21, 22]. Especially, the biased upwind finite difference scheme has better accuracy than the upwind one.

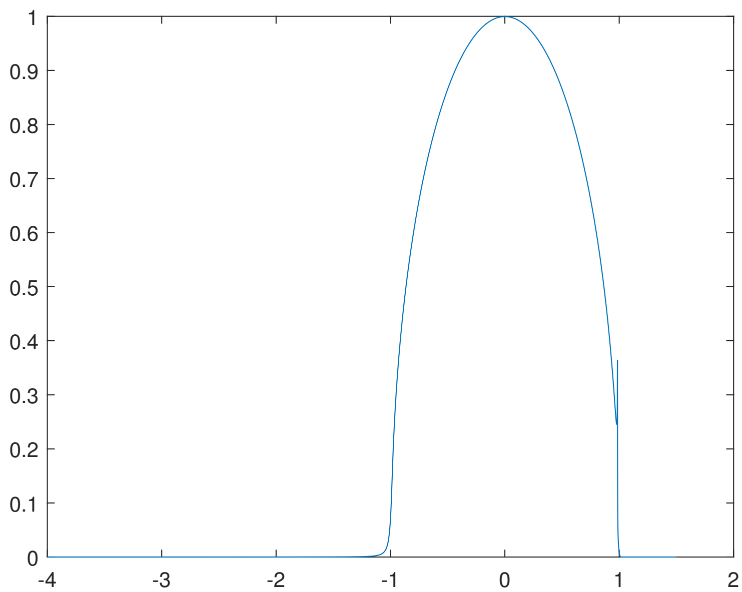

FIGURE 1. The pressure profile for $M = 200$ and $L = 10$ with $N = 4001$

4.2. **Moderate loads.** Let $M = 20$ and $L = 10$. At this situation, the maximum Hertzian dry contact pressure is 1.05 GPa for $\alpha = 1.7 \times 10^{-8}$. The results are displayed in Figure 2 and Table 3. From Table 3, the same argument can be made as the high loads.

TABLE 1. Comparison of P_s from our method and other methods

N	Upwind	Biased upwind	Results in [21, 22]	Results in [21, 22]
2001	0.3155	0.3434	$0.3167(N \approx 1793)$	$0.3656(N \approx 14335)$
4001	0.3357	0.3639	$0.3073(N \approx 3585)$	$0.3656(N \approx 14335)$

TABLE 2. Comparison of H_m from our method and other methods

N	Upwind	Biased upwind	Results in [21, 22]	Results in [21, 22]
2001	0.005472	0.005508	$0.005466(N \approx 1793)$	$0.005516(N \approx 14335)$
4001	0.005505	0.005516	$0.005502(N \approx 3585)$	$0.005516(N \approx 14335)$

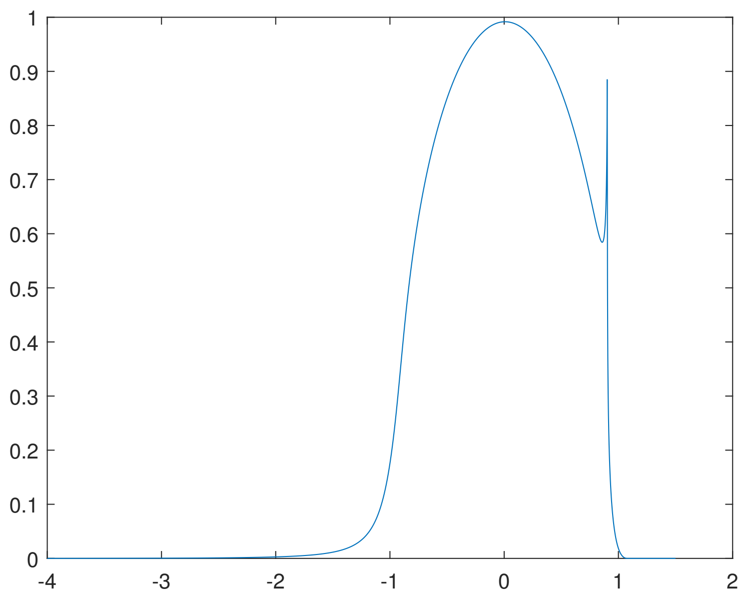

FIGURE 2. The pressure profile for $M = 20$ and $L = 10$ with $N = 4001$ by the biased upwind finite difference scheme

TABLE 3. Comparison of P_s from our method and the multilevel method [2]

N	Upwind	Biased upwind	Multilevel method [2]	Multilevel method [2]
2001	0.8210	0.8634	$0.758(N \approx 1793)$	$0.879(N \approx 114689)$
4001	0.8564	0.8848	$0.787(N \approx 3585)$	$0.879(N \approx 114689)$

5. CONCLUSION

In this paper, a fully coupled high order finite difference method is used to solve the EHL line contact problems for the first time. Numerical results show that high accurate solutions could be derived with few nodes compared to the multilevel method. Furthermore, the biased upwind finite difference scheme has a better accuracy than the upwind one. In future, we shall apply our method to the EHL point contact problems in two dimensions.

Declarations

Funding This work was supported by the National Natural Science Foundation of China (No. 11401416 and No. 51605318).

Conflicts of interest The authors declare that they have no known competing financial interests or personal relationships that could have appeared to influence the work reported in this paper.

Availability of data and material Not applicable.

Code availability Not applicable.

Authors' contributions Not applicable.

Ethics approval Not applicable.

Consent to participate Not applicable.

Consent for Publication All authors agree to publish the present work on Tribology Letters.

References

[1] B. Wu, M. Chen, T. Wu, Z. Wen, X. Jin, A simple 3-dimensional model to analyse wheel-rail adhesion under wet condition, Lubrication Science 30 (2) (2018) 45–55.

[2] C. H. Venner, Multilevel solution of the ehl line and point contact problems, Ph.D. thesis, University of Twente (1991).

[3] C. H. Venner, A. A. Lubrecht, Multilevel Methods in Lubrication, Elsevier, Amsterdam, 2000.

[4] D. Zhu, Q. Jane Wang, Elastohydrodynamic lubrication: A gateway to interfacial mechanics—review and prospect, Journal of Tribology 133 (4) (2011) 041001.

[5] B. Gustafsson, High Order Difference Methods for Time Dependent PDE, Springer-Verlag Berlin Heidelberg, 2008.

[6] H. Lu, M. Berzins, C. E. Goodyer, P. K. Jimack, High-order discontinuous galerkin method for elastohydrodynamic lubrication line contact problems, Communications in Numerical Methods in Engineering 21 (11) (2005) 643–650.

[7] E. Zargari, P. Jimack, M. Walkley, An investigation of the film thickness calculation for elastohydrodynamic lubrication problems, in: Proceedings of the 9th Conference on Numerical Methods for Fluid Dynamics, 2007.

[8] C. J. A. Roelands, Correlational aspects of the viscosity-temperature-pressure relationships of lubricating oils, Ph.D. thesis, Technical University Delft, Delft (1966).

[9] D. Dowson, G. R. Higginson, Elasto-hydrodynamic lubrication: the fundamentals of roller and gear lubrication, Pergamon Press, Oxford, 1966.

[10] P. Huang, Numerical calculation of lubrication: methods and programs, Wiley, Singapore, 2013.

[11] P. Huang, Numerical calculation of elastohydrodynamic lubrication: methods and programs, Wiley, Singapore, 2015.

[12] B. Fornberg, Calculation of weights in finite difference formulas, SIAM Review 40 (3) (1998) 685–691.

[13] W. E. Schiesser, G. W. Griffiths, A Compendium of Partial Differential Equation Models: Method of Lines Analysis with Matlab, Cambridge University Press, Cambridge, 2009.

[14] P. Saucez, W. Schiesser, A. V. Wouwer, Upwinding in the method of lines, Mathematics and Computers in Simulation 56 (2) (2001) 171 – 185.

[15] A. V. Wouwer, P. Saucez, W. Schiesser, S. Thompson, A matlab implementation of upwind finite differences and adaptive grids in the method of lines, Journal of Computational and Applied Mathematics 183 (2) (2005) 245 – 258.

[16] W. E. Schiesser, The numerical method of lines: Integration of partial differential equations, Academic Press, San Diego, 1991.

[17] S. Wu, A penalty formulation and numerical approximation of the reynolds-hertz problem of elastohydrodynamic lubrication, International Journal of Engineering Science 24 (6) (1986) 1001–1013.

[18] J. Nocedal, S. Wright, Numerical Optimization, 2nd Edition, Springer Series in Operations Research and Financial Engineering, Springer Science, 2006.

[19] M. J. D. Powell, Numerical Methods for Nonlinear Algebraic Equations, Gordon and Breach Science Publishers, 1970, Ch. A Fortran Subroutine for Solving Systems of Nonlinear Algebraic Equations, pp. 115–161.

[20] A. Petrusevich, Fundamental conclusions from the contact-hydrodynamic theory of lubrication, Izo. Acad. Nauk. SSSR (OTN) 2 (1951) 209–223.

[21] C. H. Venner, J. Bos, Effects of lubricant compressibility on the film thicknessin ehl line and circular contacts, Wear 173 (1994) 151–165.

[22] S. Ahmed, Efficient finite element simulation of full-system elastohydrodynamic lubrication problems, Ph.D. thesis, The University of Leeds (2012).

[*] School of Rail Transportation, Soochow University, Suzhou 215131, China
Email address: goodytiger@hotmail.com

[†] School of Rail Transportation, Soochow University, Suzhou 215131, China
Email address: jiaoda-wubing@163.com

[◊] School of Mathematical Sciences, Soochow University, Suzhou 215006, China
Email address: 15895443509@163.com